THE M_1 ANGULAR MOMENTS MODEL IN A VELOCITY-ADAPTIVE FRAME FOR RAREFIED GAS DYNAMICS APPLICATIONS

S. GUISSET[*], D. AREGBA[*], S. BRULL[*], AND B. DUBROCA[†]

Abstract. In the present work the M_1 angular moments model in a velocity-adaptive frame is presented for rarefied gas dynamics applications. First of all, the derivation of the angular M_1 moments model in the particles mean velocity frame is introduced. The choice of the mean velocity framework in order to enforce the Galilean invariance property of the model is highlighted. In addition, it is shown that the model rewritten in terms of the entropic variables is Friedrichs-symmetric. Also, the derivation of the associated conservation laws and the zero mean velocity condition are detailed. Secondly, a suitable numerical scheme, preserving the realisable requirement of the numerical solution for the angular M_1 moments model in the mean velocity frame is proposed. Thirdly, some numerical results obtained considering several test cases in different collisional regimes are displayed.

Key words. Angular moments models, entropy minimisation closure, Galilean invariance, HLL schemes.

AMS subject classifications. 76P, 76N, 65D, 65C.

1. Introduction. Kinetic descriptions are known to be very accurate to describe the transport of particles in rarefied gas dynamics [18], neutron transport [40], plasma physics [26, 29] or radiative transfer [3]. However, they are also known to be computationally expensive to describe most realistic physical applications. An alternative way consists in considering fluid descriptions based on averaged physical quantities. However, such macroscopic descriptions are often not sufficiently accurate. The studied particles may have an energy distribution far from the thermodynamic equilibrium so that the fluid description is not applicable. Moreover kinetic effects can be important over time scales shorter than the collisional time so that fluid simulations are insufficient and kinetic codes have to be considered to capture the physical processes. Kinetic approaches are usually limited to times and lengths much shorter than those studied with fluid simulations. It is therefore an important challenge to describe kinetic effects using reduced kinetic codes operating on fluid time scales [11, 24].

The angular moments models represent an alternative method situated in between the kinetic and the fluid models. They require computational times shorter than kinetic models and provide results with a higher accuracy than fluid models. They originate from an angular moments average [33, 36] of the kinetic equations. The idea is to keep the velocity modulus (denoted ζ in this work) as a variable. That allows consideration of the particle distributions in energy far from equilibrium, while using a simplified description of particle angular distribution. Such models are obtained by integration of the kinetic equation in angle (integration on the unit sphere). Thus a hierarchy of moments equations can be obtained. There exist several moment models whose differences come from the choice of the closure relation. In this document we consider the angular moments models [8] based on an entropy minimisation principle. The entropy minimisation problems have been widely studied in [28, 33, 35, 42, 1, 30, 43]. The underlying distribution function is given by an exponential of a polynomial function depending on the particle energy and it is therefore non negative. Moreover, these closures verify fundamental mathematical properties [28, 41, 25] such as hyperbolicity

---

[*]Institut Mathématiques de Bordeaux. Contact: sebastien.guisset@u-bordeaux.fr
[†]Laboratoire CELIA.

and entropy dissipation. However, their solutions could be rather different from the solution of the full kinetic equation. Moreover, from the numerical point of view, even if the closure is well defined, computational challenges remain. In particular, the resolution of the entropy minimisation problem can be very computationally costly and we refer to [1] for a specific treatment.

Firstly, the entropic M_1 model was introduced in the context of radiation hydrodynamics [45, 4, 9, 44, 7, 38, 39]. When writing the radiation hydrodynamics equations one needs to choose the frame in which the quantities are considered: the laboratory frame or the frame moving with the fluid. Even if the laboratory frame enables to keep the hyperbolic part of the system simple, the interaction part (coupling part) become very complex [32]. Therefore, in the case of moving fluids, one chooses the frame moving with the fluid in order to keep the source terms unaffected by the fluid motions. However this choice of framework brings non-conservative terms to the equations [32]. We refer here to [16] for a clear discussion of this point.
Secondly, the entropic M_1 model has been recently considered for the study of electron dynamics in plasmas [8, 22, 23, 21]. In these works the quantities are evaluated in the framework of ions which are considered as fixed. In this case the ion frame coincides with the laboratory frame. However, when considering the ion motion, the ion frame is different of the laboratory frame and, similarly to the case of a moving fluid in radiation hydrodynamics, ones works in the moving frame (ion frame) in order to keep the collision operator form simple. We mention here, that this case has never been investigated, considering entropic angular moments models, and its study seems particularly challenging.
In this work the non-charged particles dynamics is investigated. In agreement with the previous studies achieved in the fields of radiation hydrodynamics and plasma physics, and in order to extend the present study to more complex configurations, we choose to work in a velocity-adaptive frame considering the particle mean velocity. In addition to simplify the form of collision operators, this choice enables to decrease the computational cost since the velocity grid is centred on the particle mean velocity and its size can be greatly reduced. Also, this choice of velocity plays an important role on the Galilean invariance property of the model. This point is presented in details in this study.

In order to derive the M_1 angular moments model in the mean velocity frame, a velocity change is considered to derived the kinetic equation in a moving frame. Note, that rescaled velocity approaches are largely used in different context see [13, 5, 34] for example. However, the numerical treatment of the additional terms which appear when considering such a procedure on the kinetic equation can be challenging. In [12], in the context of granular flows, a numerical algorithm based on a relative energy scaling is proposed. Then, a clever de-coupling with the hydrodynamics equation is used to avoid the problems related to the change of scales in velocity variables. Significant results on the derivation of Galilean invariant minimum entropy systems have been obtained in [25]. It has been shown that polynomials weight functions growing super-quadratically at infinity lead to unusable hyperbolic moment systems. Indeed, in this case equilibrium states are boundary points of the admissible set with possible singular fluxes [25]. In addition it has also been shown that non-polynomial weight function can not be used without losing the Galilean invariance property of the moments systems. Therefore, one understands here the difficulty in deriving adapted Galilean invariant reduced models. We also mention [20, 31] where this issue is addressed.

The present study is original for two main reasons. First of all, contrarily to the previous works, angular moments are considered. The integration of the kinetic equation is only performed in angle (on the unit sphere) while the velocity modulus is kept as a variable. This partial integration leads to angular moments models which do not suffer of the restrictions presented in [25]. However, it can be shown that these resulting angular moments models are not Galilean invariant since they are not invariant by translational transformations. Therefore, the second original idea presented here to surpass this major drawback, is to work in the framework of the particles mean velocity. In this work, it is shown that this choice of velocity origin framework enables to recover the invariance property when considering translational transformations. Therefore, in this paper, a Galilean invariant reduced model is presented in the context of rarefied gas dynamics.

The plan of this study is the following. First of all, the derivation of the angular M_1 moments model in the mean velocity frame is introduced. The choice of the mean velocity framework in order to enforce the Galilean invariance property of the model is highlighted. In addition, it is shown that the model rewritten in terms of the entropic variables is Friedrichs-symmetric. Also, the derivation of the associated conservation laws and the zero mean velocity condition are detailed. Secondly, a suitable numerical scheme, preserving the realisability requirement of the numerical solution for the angular M_1 moments model in the mean velocity frame is proposed. Thirdly, some numerical results obtained considering several test cases in different collisional regimes are displayed. Finally, some conclusion and perspectives are given.

2. Derivation of the model. Velocity change of variables procedures are used in various contexts (see [13, 12, 5, 34] for example) and can enable the simplification of a collisional operator form or the reduction of the velocity grid size used for numerical applications. In the context of angular moments models [8], it will be seen in the next section that moving frame formulations play an important role in enforcing the Galilean invariance property. In order to explain in details this point, in this section we introduce the kinetic formulation in a moving frame from which the M_1 angular moments model studied is derived.

2.1. The kinetic equation in a velocity-adaptive frame. We start considering the following kinetic equation written in the laboratory framework

$$(2.1) \qquad \partial_t f(\alpha) + div_x(v f(\alpha)) = C(f(\alpha)),$$

where f represents the particle distribution function and $\alpha = (t, x, v) \in \mathbb{R}_t^+ \times \mathbb{R}_x^3 \times \mathbb{R}_v^3$. The form of the collisional operator C is not detailed here but only the properties used in this study will be detailed.

PROPOSITION 2.1. *The kinetic equation (2.1) written in a velocity-adaptive framework writes*

$$(2.2) \qquad \partial_t g(t, x, c) + div_x((c + u) g(t, x, c))$$
$$- div_c \Big[(\partial_t u + \partial_x u (c + u)) g(t, x, c) \Big] = C(g(t, x, c)),$$

where the new velocity c is defined by

$$c = v - u(t, x),$$

with u a relative velocity which needs be specified.

Remark: The term $(\partial_x u)$ is a second order tensor defined by

$$(\partial_x u)_{ij} = \partial_{x_j} u_i.$$

Proof. In this case the transformation is a velocity shift

$$f(t, x, v) = f(t, x, c + u(t, x)) \equiv g(t, x, c),$$

and one directly obtains

$$df = dg - \sum_k (\partial_{c_k} g) du_k,$$

where we use $d = \partial_t$ and $d = \partial_{x_i}$. Therefore from

$$\partial_t f + \sum_i v_i \partial_{x_i} f = 0,$$

it follows that

$$\partial_t g + \sum_i (c_i + u_i) \partial_{x_i} g - \sum_k \partial_{c_k} g (\partial_t u_k + \sum_i (c_i + u_i) \partial_{x_i} u_k) = 0,$$

which rewrites

$$\partial_t g + \sum_i \partial_{x_i} ((c_i + u_i) g) - \sum_k \partial_{c_k} ((\partial_t u_k + \sum_i (c_i + u_i) \partial_{x_i} u_k) g) = 0,$$

giving the result (2.2).
□

Eq.(2.2) is used in the next sections to derive the angular M_1 moments model in a velocity-adaptive frame. Of course, an additional evolution equation is required to compute the velocity u. In this work, the velocity u is chosen as the particles mean velocity in the fixed frame (laboratory frame). This choice enables the reduction of the size of the velocity grids and plays an important role in enforcing the Galilean invariance property of the angular M_1 model. This point is presented in details in the next sections. In order to derive the evolution equation for u, the kinetic equation (2.1) is integrated in velocity. This leads to the following conservation laws

(2.3) $$\partial_t n + div_x(nu) = 0,$$

$$\partial_t (nu) + div_x \left(\int_v f v \otimes v dv \right) = 0.$$

Remark: The divergence of a second order tensor $\bar{\bar{A}}$ results in a vector defined by

$$(div_x \bar{\bar{A}})_i = \sum_j \partial_{x_j} A_{ij}.$$

Injecting the following expansion into (2.3)

$$v \otimes v = (v - u) \otimes (v - u) + (v - u) \otimes u + u \otimes (v - u) + u \otimes u,$$

and by using the following identities

$$\int_v u \otimes u f dv = n u \otimes u,$$

$$\int_v u \otimes (v-u) f dv = u \otimes \int_v (v-u) f dv = 0,$$

$$\int_v (v-u) \otimes u f dv = \int_v (v-u) f dv \otimes u = 0,$$

one obtains the evolution equation for u expressed in the new frame quantities

$$(2.4) \qquad \partial_t(nu) + div_x(nu \otimes u) + div_x\left(\int_v g(c)c \otimes c dc\right) = 0,$$

where

$$n = \int_c g(c) dc.$$

The equations (2.3) and (2.4) will be used to compute the relative velocity u at each time step.

2.2. M_1 angular moments model in a moving frame. The M_1 angular moments model in a moving frame is derived by performing an angular moments extraction of the kinetic equation (2.2). One defines the following three first angular moments of the distribution function g

$$g_0(\zeta) = \zeta^2 \int_{S^2} g(\Omega,\zeta) d\Omega, \;\; g_1(\zeta) = \zeta^2 \int_{S^2} g(\Omega,\zeta)\Omega d\Omega, \;\; g_2(\zeta) = \zeta^2 \int_{S^2} g(\Omega,\zeta)\Omega \otimes \Omega d\Omega,$$

where S^2 is the unit sphere.
The complete derivation of the M_1 angular moments model in a moving frame is presented in appendix. Removing the collisional operators contribution, this model reads

$$(2.5) \quad \begin{cases} \partial_t g_0 + div_x(\zeta g_1 + u g_0) - \partial_\zeta\left(\dfrac{du}{dt}\cdot g_1 + \zeta\partial_x u : g_2\right) = 0, \\[2mm] \partial_t g_1 + div_x(\zeta g_2 + u \otimes g_1) - \partial_\zeta\left(g_2\dfrac{du}{dt} + \zeta g_3 \partial_x u\right) \\[2mm] \qquad\qquad\qquad + \dfrac{g_0 Id - g_2}{\zeta}\dfrac{du}{dt} + \left((\partial_x u)g_1 - g_3(\partial_x u)\right) = 0, \end{cases}$$

where $\dfrac{du}{dt}$ is defined as

$$\frac{du}{dt} = \partial_t u + (\partial_x u)u,$$

and the third order moments g_3 as

$$(2.6) \qquad g_3(\zeta) = \zeta^2 \int_{S^2} g(\Omega,\zeta)\Omega \otimes \Omega \otimes \Omega d\Omega.$$

Remark: The term $(\partial_x u)g_1$ represents the product of the second order tensor $(\partial_x u)$ with the vector g_1 and results in a vector defined by

$$((\partial_x u)g_1)_i = \sum_j (\partial_{x_j} u_i)g_{1j}.$$

The term $g_3(\partial_x u)$ represents the product of the third order tensor g_3 with the second order tensor $(\partial_x u)$ and results in a vector defined by

$$(g_3(\partial_x u))_i = \sum_{j,k} g_{3ijk}(\partial_{x_k} u_j).$$

The term $\partial_x u : g_2$ represents the twice tensor contraction of the second order tensor $(\partial_x u)$ with the second order tensor g_2 and results in a scalar defined by

$$\partial_x u : g_2 = \sum_{i,j}(\partial_{x_j} u_i) : g_{2ij}.$$

The evolution law (2.4) expressed in terms of the angular moments rewrites

$$(2.7) \qquad \partial_t(nu) + div_x(nu \otimes u) + div_x\Big(\int_0^{+\infty} g_2(\zeta)\zeta^2 d\zeta\Big) = 0.$$

In order to close the system (2.5), the higher order moments g_2 and g_3 must be expressed in terms of g_0 and g_1. Following [8] and the references therein, the M_1 closure is considered. This closure relation originates from an entropy minimisation principle [28, 33]. The underlying distribution function g is obtained as a solution of the following minimisation problem

$$(2.8) \quad \min_{g \geq 0}\{ \; \mathcal{H}(g) \; / \; \forall \zeta \in \mathbb{R}^+, \; \zeta^2 \int_{S^2} g(\Omega, \zeta)d\Omega = g_0(\zeta), \; \zeta^2 \int_{S^2} g(\Omega, \zeta)\Omega d\Omega = g_1(\zeta) \; \},$$

where $\mathcal{H}(g)$ is the angular entropy defined by

$$\mathcal{H}(g) = \zeta^2 \int_{\mathbb{S}^2} (g \; \ln \; g \; - \; g)d\Omega.$$

The solution of (2.8) writes [28, 10]

$$(2.9) \qquad g(\Omega, \zeta) = \exp(\; a_0(\zeta) + a_1(\zeta).\Omega \;),$$

where $a_0(\zeta)$ is a scalar and $a_1(\zeta)$ a real valued vector. The coefficients a_0 and a_1 are the Lagrange multipliers associated to entropy minimisation problem (2.8), to a certain extent they represent the moments g_0 and g_1, and we refer to [30, 28] and the references therein for more details on minimum entropic closures. Then extending the ideas of [10, 8, 28] one can show that the closure relation for g_2 is given by

$$(2.10) \qquad g_2 = g_0\Big(\frac{3\chi(\alpha) - 1}{2} \frac{g_1}{|g_1|} \otimes \frac{g_1}{|g_1|} + \frac{1 - \chi(\alpha)}{2}Id\Big),$$

where

$$(2.11) \qquad \chi(\alpha) = \frac{1 + |\alpha|^2 + |\alpha|^4}{3}, \qquad\qquad \alpha = g_1/g_0.$$

Similarly the higher order moment g_3 reads

$$(2.12) \qquad g_3 = \Big(\frac{3|g_1| - \chi_2 g_0}{2}\Big)\frac{g_1}{|g_1|} \otimes \frac{g_1}{|g_1|} \otimes \frac{g_1}{|g_1|} + \frac{\chi_2 g_0 - |g_1|}{2}\Big(\frac{g_1}{|g_1|} \vee Id\Big),$$

with

$$\chi_2(\alpha) = \frac{3|\alpha| - |\alpha|^3 + 3|\alpha|^5}{5},$$

and

$$
\begin{aligned}
\frac{g_1}{|g_1|} \vee Id = &\frac{g_1}{|g_1|} \otimes e_1 \otimes e_1 + e_1 \otimes \frac{g_1}{|g_1|} \otimes e_1 + e_1 \otimes e_1 \otimes \frac{g_1}{|g_1|}\\
&+ \frac{g_1}{|g_1|} \otimes e_2 \otimes e_2 + e_2 \otimes \frac{g_1}{|g_1|} \otimes e_2 + e_2 \otimes e_2 \otimes \frac{g_1}{|g_1|}\\
&+ \frac{g_1}{|g_1|} \otimes e_3 \otimes e_3 + e_3 \otimes \frac{g_1}{|g_1|} \otimes e_3 + e_3 \otimes e_3 \otimes \frac{g_1}{|g_1|}.
\end{aligned}
$$

Before studying the models properties, the realisability conditions associated to the model (2.5) are introduced

$$(2.13) \qquad \mathcal{A} = \Big((g_0, g_1) \in \mathbb{R}^2, \ g_0 \geq 0, \ |g_1| \leq g_0\Big).$$

Since the distribution function g is a nonnegative quantity the realisability conditions (2.13) naturally needs to be satisfied. In addition, these conditions are related to the existence of a nonnegative distribution function from which the angular moments can be derived [36].

3. Model properties. In this section the main properties of the angular M_1 model in a moving frame (2.5)-(2.7) are presented. It is first proved that the choice of working in the mean velocity frame enables to ensure the Galilean invariance property of the model. Secondly it is shown that this model, rewritten in terms of entropic variables, is Friedrichs-symmetric. Finally, the derivation of the conservation laws is detailed.

3.1. Galilean invariance property. Galilean invariance is a fundamental feature of the Boltzmann equation. Following [25], we start defining translational and rotational transformations. For any vector $s \in \mathbb{R}^d$ and any rotation matrix $R \in SO(d)$

$$(\mathcal{T}_s f)(v) = f(v - s), \qquad (\mathcal{T}_R f)(v) = f(Rv), \qquad v \in \mathbb{R}^d.$$

The following translational and rotational invariance properties of the collisional operator C are considered

$$(3.1) \qquad \mathcal{T}_s C(f) = C(\mathcal{T}_s(f)), \qquad \mathcal{T}_R C(f) = C(\mathcal{T}_R(f)).$$

Note that the Boltzmann collision operator or the BGK collision operator [19] satisfy such properties. Using equation (3.1) the Galilean invariance property of the kinetic equation (2.1) can be shown. Indeed, the reference coordinates system (t, x, v) and a new set of coordinates $(t, \tilde{x}, \tilde{v})$ can be linked by the following relations

$$(3.2) \qquad \tilde{x} = Rx - st, \qquad \tilde{v} = Rv - s,$$

for any constant vector $s \in \mathbb{R}^d$. Distribution function $\tilde{f}$ in the moving frame is defined as

$$\tilde{f}(t, \tilde{x}, \tilde{v}) = f(t, x, v).$$

Consequently the following relations can be derived

$$\partial_t f(t,x,v) = \partial_t \tilde{f}(t,\tilde{x},\tilde{v}) - s.\partial_x \tilde{f}(t,\tilde{x},\tilde{v}), \qquad \partial_x f(t,x,v) = R\partial_{\tilde{x}}\tilde{f}(t,\tilde{x},\tilde{v}).$$

Therefore using (2.1), it follows that $\tilde{f}$ satisfies

$$(3.3) \qquad \qquad \partial_t \tilde{f}(t,\tilde{x},\tilde{c}) + div_{\tilde{x}}(\tilde{v}\tilde{f}(t,\tilde{x},\tilde{c})) = C(\tilde{f}(t,\tilde{x},\tilde{c})),$$

which shows the Galilean invariance of (2.1).

The same property cannot be directly obtained when considering the M_1 angular moments model (2.5)-(2.7). Indeed, when integrating (2.1) on the unit sphere and applying the change of variables (3.2) lead to inconvenient nonlinear terms and we are not able to show that the form of the M_1 model is invariant by translational transformation. In order to overcome this drawback, in this study, we propose to not derive the M_1 angular moments model from the kinetic equation (2.1) but from the kinetic equation (2.2) which is expressed in a mobile reference frame. In particular, in this work the velocity u used in (2.2) is chosen as the particles mean velocity defined by

$$(3.4) \qquad \qquad u = \frac{1}{n}\int_{\mathbb{R}^3} f(v)v dv.$$

In order to show the advantage in deriving the M_1 angular moments model from the kinetic equation (2.2), the kinetic equation (3.3) is rewritten in its mean velocity frame. This second kinetic equation expressed in a velocity-adaptive frame reads

$$(3.5) \qquad \partial_t \tilde{g}(t,\tilde{x},\tilde{c}) + div_{\tilde{x}}((\tilde{c}+\tilde{u})\tilde{g}(t,\tilde{x},\tilde{c}))$$
$$- div_{\tilde{c}}\big[(\partial_t \tilde{u} + \partial_{\tilde{x}}\tilde{u}(\tilde{c}+\tilde{u}))\tilde{g}(t,\tilde{x},\tilde{x})\big] = C(\tilde{g}(t,\tilde{x},\tilde{c})),$$

where

$$(3.6) \qquad \qquad \tilde{u} = \frac{1}{n}\int_{\mathbb{R}^3} \tilde{f}(\tilde{v})\tilde{v}d\tilde{v}.$$

The key point which will be useful when considering angular moments models is the relation between the two kinetic equations (2.2) and (3.5). Indeed, the two relative velocities u and $\tilde{u}$ are linked through the following relation

$$(3.7) \qquad \qquad \tilde{u} = Ru - s.$$

Therefore, we propose to consider the following change of variable

$$(3.8) \qquad \qquad \tilde{x} = Rx - st, \quad \tilde{c} = Rc, \quad \tilde{u} = Ru - s.$$

Indeed, by injecting the change of variable (3.7)-(3.8) into (2.2) and using the following relations

$$(3.9) \qquad \qquad \begin{aligned} \partial_t u &= {}^tR(\partial_t \tilde{u} - (\partial_{\tilde{x}}\tilde{u})s), \\ \partial_x u &= {}^tR(\partial_{\tilde{x}}\tilde{u})R, \end{aligned}$$

and

$$(3.10) \qquad \qquad \begin{aligned} \partial_t g &= \partial_t \tilde{g} - (\partial_{\tilde{x}}\tilde{g})s, \\ \partial_x g &= (\partial_{\tilde{x}}\tilde{g})R, \\ \partial_c g &= (\partial_{\tilde{c}}\tilde{g})R, \end{aligned}$$

a direct calculation enables to recover equation (3.5). The relationships between the different studied frameworks are summarised on Fig 3.1. The starting point is the kinetic equation (2.1) expressed in the fixed frame, denoted A_0. Since this kinetic equation is Galilean invariant, one obtains (3.3) denoted B_0, by using (3.2). Secondly, the kinetic equation in a velocity-adaptive frame (2.2) denoted A has been derived. In the present case u is the particles mean velocity defined in (3.4). The same procedure can be applied on (3.3) to obtain (3.5), denoted B. Finally, one remarks that (2.2) and (3.5), denoted A and B are linked by the change of variable (3.8). The change

$$\tilde{x} = Rx - st$$
$$\tilde{v} = Rv - s$$

A_0 : fixed frame $\qquad\longrightarrow\qquad$ B_0 : Translation frame

$$\partial_t f + div_x(vf) = C(f) \qquad\qquad \partial_t \tilde{f} + div_{\tilde{x}}(\tilde{v}\tilde{f}) = C(\tilde{f})$$

$$c = v - u(t,x) \qquad\qquad\qquad\qquad\qquad \tilde{c} = \tilde{v} - \tilde{u}(t,\tilde{x})$$

$$nu(t,x) = \int_v fv\,dv \qquad\qquad\qquad\qquad n\tilde{u}(t,\tilde{x}) = \int_{\tilde{v}} \tilde{f}\tilde{v}\,d\tilde{v}$$

A : velocity-adaptive frame $\qquad\longrightarrow\qquad$ B : Translation velocity-adaptive frame

$$\partial_t g + div_x((c+u)g) \qquad\qquad \tilde{x} = Rx - st \qquad \partial_t \tilde{g} + div_{\tilde{x}}((\tilde{c}+\tilde{u})\tilde{g})$$
$$\tilde{c} = Rc$$
$$-div_c\big[(\partial_t u + \partial_x u(c+u))g\big] = C(g) \qquad \tilde{u} = Ru - s \qquad -div_{\tilde{c}}\big[(\partial_t \tilde{u} + \partial_{\tilde{x}}\tilde{u}(c+\tilde{u}))\tilde{g}\big] = C(\tilde{g})$$
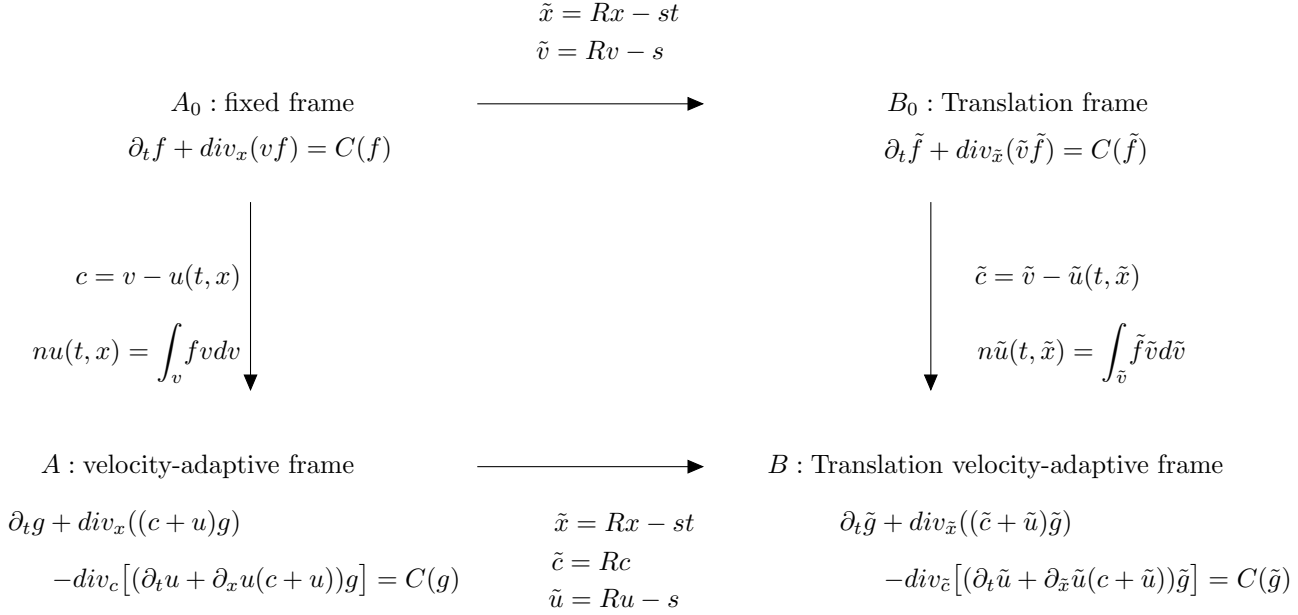
Fig. 3.1: Diagram presenting the relations between the different frames

of variables (3.8) makes the link between equations (2.2) and (3.5) relevant when considering angular moments models. Indeed, this change of variable also enables to link the angular M_1 model derived from the kinetic equation (2.2) to the angular M_1 model derived from the kinetic equation (3.5). This point is detailed in the following result.

THEOREM 3.1. *(Galilean invariance property)*
The form of the M_1 angular moments model (2.5) expressed in the mean velocity frame is invariant by rotational and translational transformations.

Proof. Before showing the Galilean invariance property of the M_1 angular moments model (2.5), we define the quantities in the new frame. Consider the velocity modulus $\tilde{\zeta}$ and $\tilde{\Omega}$ the angular direction in the velocity-adaptive frame

$$\tilde{\zeta} = |\tilde{c}|, \qquad \tilde{c} = \tilde{\zeta}\tilde{\Omega},$$

we define the two first angular moments $\tilde{g}_0$ and $\tilde{g}_1$ in the velocity-adaptive frame

$$\tilde{g}_0 = \tilde{\zeta}^2 \int_{\tilde{S}_2} \tilde{g}(t,\tilde{x},\tilde{c})d\tilde{\Omega}, \qquad \tilde{g}_1 = \tilde{\zeta}^2 \int_{\tilde{S}_2} \tilde{g}(t,\tilde{x},\tilde{c})\tilde{\Omega}d\tilde{\Omega}.$$

Using the fact that

(3.11) $$\tilde{\zeta} = \zeta, \qquad \tilde{\Omega} = R\Omega,$$

and the equations (3.10), the following relations can be derived

(3.12)
$$\begin{aligned}
\tilde{g}_0 &= g_0, \\
\partial_t g_0 &= \partial_t \tilde{g}_0 - \partial_{\tilde{x}} \tilde{g}_0 s, \\
\partial_x g_0 &= \partial_{\tilde{x}} \tilde{g}_0 R, \\
\partial_\zeta g_0 &= \partial_{\tilde{\zeta}} \tilde{g}_0,
\end{aligned}$$

and

(3.13)
$$\begin{aligned}
g_1 &= R\tilde{g}_1, \\
\partial_t g_1 &= {}^t R(\partial_t \tilde{g}_1 - \partial_{\tilde{x}} \tilde{g}_1 s), \\
\partial_x g_1 &= {}^t R \partial_{\tilde{x}} \tilde{g}_1 R, \\
\partial_\zeta g_1 &= {}^t R \partial_{\tilde{\zeta}} \tilde{g}_1.
\end{aligned}$$

Using the definition of $\tilde{g}_2$, we remark that

(3.14)
$$\begin{aligned}
\tilde{g}_2 &= \tilde{\zeta}^2 \int_{\tilde{S}_2} \tilde{g}(t, \tilde{x}, \tilde{c}) \tilde{\Omega} \otimes \tilde{\Omega} d\tilde{\Omega} \\
&= \zeta^2 \int_{\tilde{S}_2} \tilde{g}(t, \tilde{x}, \tilde{c}) R\tilde{\Omega} \otimes \tilde{\Omega}\, {}^t R d\tilde{\Omega}.
\end{aligned}$$

Then injecting (3.12)-(3.13) into the first equation of (2.5) and using (3.14) and (3.9) a direct calculation gives

$$\partial_t \tilde{g}_0 + div_x(\tilde{\zeta}\tilde{g}_1 + \tilde{u}\tilde{g}_0) - \partial_{\tilde{\zeta}}\left(\frac{d\tilde{u}}{dt}.\tilde{g}_1 + \tilde{\zeta}\partial_{\tilde{x}}\tilde{u} : \tilde{g}_2\right) = 0.$$

In order to deal with the second equation of (2.5), we remark that using (3.11) the ijk^{th} component of the higher order moments g_3 defined in (2.6) rewrites

(3.15) $$g_{3ijk} = \sum_{l,m,n} \tilde{\zeta}^2 \int_{\tilde{S}_2} {}^t R_{il}\, {}^t R_{jm}\, {}^t R_{kn} (\tilde{\Omega} \otimes \tilde{\Omega} \otimes \tilde{\Omega})_{lmn} d\tilde{\Omega}.$$

Therefore, using (3.14) and (3.15) a direct calculation gives

(3.16) $$div_x g_2 = {}^t R\, div_{\tilde{x}} \tilde{g}_2,$$

and

(3.17) $$g_3 \partial_x u = {}^t R\, \tilde{g}_3 \partial_x \tilde{u}.$$

Consequently injecting (3.12)-(3.13) into the second equation of (2.5) and using the relations (3.9)-(3.16) and (3.17), one obtains

$$\begin{cases}
\partial_t \tilde{g}_1 + div_{\tilde{x}}(\tilde{\zeta}\tilde{g}_2 + \tilde{u} \otimes \tilde{g}_1) - \partial_{\tilde{\zeta}}\left(\tilde{g}_2 \frac{d\tilde{u}}{dt} + \tilde{\zeta}\tilde{g}_3 \partial_{\tilde{x}}\tilde{u}\right) \\
\qquad\qquad\qquad + \frac{\tilde{g}_0 Id - \tilde{g}_2}{\tilde{\zeta}} \frac{d\tilde{u}}{dt} + ((\partial_{\tilde{x}}\tilde{u})\tilde{g}_1 - \tilde{g}_3 \partial_{\tilde{x}}\tilde{u}) = 0.
\end{cases}$$

□

3.2. Symmetrization property. In this section it is shown that the M_1 model in a moving frame (2.5)-(2.7) written in terms of the entropic variables is Friedrichs symmetric. Following [28], the M_1 model in a moving frame (2.5) can be rewritten in terms of the entropic variables a_0 and a_1. This procedure is sometimes called a Godunov's symmetrisation [17].

THEOREM 3.2. *The M_1 model in a moving frame (2.5) written in terms of the variables a_0 and a_1 is Friedrichs symmetric.*

Remark: We mention here that this property is not shown for the complete system (2.5)-(2.7), we only consider the system (2.5) for a given u with enough regularity neglecting the coupling. The demonstration to the general model seems particularly challenging.

Proof. Setting

$$^t m = (1, \Omega), \qquad ^t \alpha = (\alpha_0, \alpha_1),$$

the distribution function (2.9) reads

$$g(t, x, \zeta, \Omega) = \exp(\alpha . m),$$

and the solution of (2.5)-(2.10)-(2.12) writes

$$^t(g_0, g_1) = \langle \zeta^2 \exp(\alpha . m) m \rangle,$$

where the notation $\langle . \rangle$ refers to the angular integration on the unit sphere. Consequently, after a direct calculation, the M_1 angular moments model in a moving frame (2.5) rewrites

$$(3.18) \quad A_0(\alpha) \partial_t \begin{pmatrix} \alpha_0 \\ \alpha_1 \end{pmatrix} + \sum_j A_j(\alpha) \partial_{x_j} \begin{pmatrix} \alpha_0 \\ \alpha_1 \end{pmatrix} + B(\alpha) \partial_\zeta \begin{pmatrix} \alpha_0 \\ \alpha_1 \end{pmatrix} + S(x, \zeta, \alpha) = \begin{pmatrix} 0 \\ 0 \end{pmatrix},$$

where

$$A_0(\alpha) = < \exp(\alpha . m) \begin{pmatrix} 1 & ^t\Omega \\ \Omega & \Omega \otimes \Omega \end{pmatrix} >,$$

$$A_j(\alpha) = < (\zeta \Omega_j + u_j) \exp(\alpha . m) \begin{pmatrix} 1 & ^t\Omega \\ \Omega & \Omega \otimes \Omega \end{pmatrix} >,$$

$$B(\alpha) = < -(\zeta^2 \frac{du}{dt} . \Omega + \zeta^3 \partial_x u : \Omega \otimes \Omega) \exp(\alpha . m) \begin{pmatrix} 1 & ^t\Omega \\ \Omega & \Omega \otimes \Omega \end{pmatrix} >,$$

and

$$S(x, \zeta, \alpha) = \begin{pmatrix} (div_x u) g_0 - \dfrac{2}{\zeta} \dfrac{du}{dt} . g_1 - 3 \partial_x u : g_2 \\ (\partial_x u) g_1 - \dfrac{2}{\zeta} g_2 \dfrac{du}{dt} - 3 g_3 \partial_x u + \dfrac{g_0 Id - g_2}{\zeta} \dfrac{du}{dt} + ((\partial_x u) g_1 - g_3 (\partial_x u)) \end{pmatrix}.$$

Since $A_0(\alpha)$ is a positive-definite symmetric matrix and $A_j(\alpha)$ and $B(\alpha)$ are symmetric matrices, one obtains that the system (3.18) is Friedrichs-symmetric [14, 2]. □

3.3. Conservation laws. In this section the derivation of the conservation laws derived from the angular M_1 model in a moving frame (2.5) is detailed.

Before deriving the mass and energy conservation equations, we point out that in this work the velocity u is chosen as the particles mean velocity. Therefore, in the considered framework the mean velocity is equal to zero. This point is expressed by the following condition

$$(3.19) \qquad \int_0^{+\infty} g_1(t, x, \zeta)\zeta d\zeta = 0.$$

Multiplying the second equation of (2.5) by ζ and integrating in ζ, one shows using Green's formula that all the terms vanish two by two and that condition (3.19) is preserved over times.

The derivation of the mass conservation equation can be directly obtained by direct integration in ζ. Indeed, integrating the first equation of (2.5) in ζ, one obtains

$$(3.20) \qquad \partial_t n + div_x(nu) = 0,$$

where condition (3.19) has been used.

In order to derive the energy conservation equation, one starts multiplying the first equation of (2.5) by $\dfrac{m}{2}\zeta^2$ and integrate in ζ to obtain the following internal energy equation

$$(3.21) \qquad \partial_t\Big(\frac{1}{2}\int_0^{+\infty} g_0\zeta^2 d\zeta\Big) + div_x\Big(\frac{1}{2}\int_0^{+\infty} g_1\zeta^3 d\zeta + u\frac{1}{2}\int_0^{+\infty} g_0\zeta^2 d\zeta\Big)$$
$$+ \Big(\partial_x u : \int_0^{+\infty} g_2\zeta^2 d\zeta\Big) = 0.$$

One notices that since the mean velocity frame is considered, only an equation on the internal energy is obtained. The kinetic energy equation is derived from the evolution equation (2.7) and writes

$$(3.22) \qquad \partial_t(nu^2) + div_x\Big(\frac{nu^2}{2}u\Big) + u.div_x\Big(\int_0^{+\infty} g_2\zeta^2 d\zeta\Big) = 0.$$

The energy conservation equation is directly obtained by summing equation (3.21) with equation (3.22).

4. Numerical scheme. In this part an appropriate numerical scheme is proposed for the M_1 model in a moving framework in an one dimensional spatial geometry considering a standard BGK collision operator [19]. In this case, the collisional operator $C(f)$ used in (2.1) is specified

$$C(f) = \frac{1}{\tau}(M_f - f),$$

with

$$M_f(v) = \frac{n}{(2\pi T)^{3/2}} \exp\Big(-\frac{(v-u)^2}{2T}\Big),$$

and τ is a collisional parameter which is fixed depending of the collisional regime studied. In this case the M_1 model in a moving framework (2.5) writes

$$
(4.1) \quad \begin{cases} \partial_t g_0 + \partial_x(\zeta g_1 + u g_0) - \partial_\zeta\left(\dfrac{du}{dt}g_1 + \zeta(\partial_x u)g_2\right) = \dfrac{1}{\tau}(M_{g_0} - g_0), \\[2mm] \partial_t g_1 + \partial_x(\zeta g_2 + u g_1) - \partial_\zeta\left(\dfrac{du}{dt}g_2 + \zeta(\partial_x u)g_3\right) + \dfrac{du}{dt}\dfrac{g_0 - g_2}{\zeta} \\[4mm] \hspace{5cm} + (\partial_x u)(g_1 - g_3) = -\dfrac{1}{\tau}g_1, \end{cases}
$$

where

$$
M_{g_0} = 4\pi\zeta^2 \frac{n}{(2\pi T)^{3/2}} \exp\left(-\frac{\zeta^2}{2T}\right).
$$

4.1. Derivation of the numerical scheme. In order to derive a suitable numerical scheme for the model (4.1) which preserves the admissibility of the solution, the different terms of (4.1) are studied separately. Then the admissibility requirement of the complete scheme is shown under a reduced CFL condition.

Step 1: the first intermediate state is the following

$$
(4.2) \quad \begin{cases} \partial_t g_0 + \partial_x(\zeta g_1 + u g_0) = 0, \\ \partial_t g_1 + \partial_x(\zeta g_2 + u g_1) = 0. \end{cases}
$$

In order to derive a numerical scheme preserving the realisability of the numerical solution, we consider an underlying kinetic model from which the system (4.2) can be derived by direct angular moments extraction

$$
(4.3) \quad \partial_t F(t, x) + \partial_x(a(x)F(t, x)) = 0,
$$

with $F = \zeta^2 g$, $a(x) = \zeta\mu + u(x)$ and $\mu \in [-1, 1]$. Note that μ is the angular variable in the case of one space dimension.

A natural conservative numerical scheme is proposed for the kinetic equation (4.3)

$$
(4.4) \quad \frac{F_i^{n+1} - F_i^n}{\Delta t} + \frac{h_{i+1/2}^n - h_{i-1/2}^n}{\Delta x} = 0,
$$

with

$$
h_{i+1/2}^n = a_{i+1/2}^- F_{i+1}^n + a_{i+1/2}^+ F_i^n,
$$

and $a^{\pm} = \dfrac{1}{2}(a \pm |a|)$.

Rewriting equation (4.4) as a convex combination

$$
(4.5) \quad \begin{aligned} F_i^{n+1} = {}& F_i^n\left(1 - \frac{\Delta t}{2\Delta x}(a_{i+1/2} - a_{i-1/2}) - \Delta t\frac{|a_{i+1/2}| + |a_{i-1/2}|}{2\Delta x}\right) \\ & + F_{i+1}^n\frac{2\Delta t}{\Delta x}\left(|a_{i+1/2}| - a_{i+1/2}\right) \\ & + F_{i-1}^n\frac{2\Delta t}{\Delta x}\left(|a_{i-1/2}| - a_{i-1/2}\right), \end{aligned}
$$

it follows that the positivity of the numerical distribution function is ensured under the following CFL condition

$$(4.6) \qquad \Delta t_1 \leq \frac{\Delta x}{2||u||_\infty + \zeta}.$$

The numerical scheme (4.5) rewrites on the following viscous form

$$(4.7) \qquad \frac{F_i^{n+1} - F_i^n}{\Delta t} + \frac{a_{i+1/2}F_{i+1}^n + (a_{i+1/2} - a_{i-1/2})F_i^n - a_{i-1/2}F_{i-1}^n}{2\Delta x}$$
$$- \frac{|a_{i+1/2}|F_{i+1}^n - (|a_{i+1/2}| + |a_{i-1/2}|)F_i^n + |a_{i-1/2}|F_{i-1}^n}{2\Delta x} = 0.$$

The angular integration can not be directly performed on the scheme (4.7) because of the angular variable μ which appears in the term $|a|$ in the numerical viscosity. Therefore we modify (4.7) and consider the following scheme which is suitable for the angular integration.

$$(4.8) \qquad \frac{F_i^{n+1} - F_i^n}{\Delta t} + \frac{a_{i+1/2}F_{i+1}^n + (a_{i+1/2} - a_{i-1/2})F_i^n - a_{i-1/2}F_{i-1}^n}{2\Delta x}$$
$$- ||a||_\infty \frac{F_{i+1}^n - 2F_i^n + F_{i-1}^n}{2\Delta x} = 0.$$

Remark: Considering (4.8), one observes that the numerical viscosity of the scheme is increased in order to enable the angular integration.Therefore the numerical scheme still preserves the nonnegativity of the numerical solution under CFL condition (4.6).

The angular integration of the scheme (4.8) leads to a natural discretisation for the intermediate state (4.2)

$$\frac{g_{0i}^{n+1} - g_{0i}^n}{\Delta t} + \frac{(\zeta g_{1i+1}^n + u_{i+1/2}g_{0i+1}^n) + ((\zeta g_{1i}^n + u_{i+1/2}g_{0i}^n)}{2\Delta x}$$
$$- \frac{(\zeta g_{1i}^n + u_{i-1/2}g_{0i}^n)) - (\zeta g_{1i}^n + u_{i-1/2}g_{0i-1}^n)}{2\Delta x} - (\zeta + ||u||_\infty)\frac{g_{0i+1}^n - 2g_{0i}^n + g_{0i-1}^n}{2\Delta x} = 0,$$

(4.9)
$$\frac{g_{1i}^{n+1} - g_{1i}^n}{\Delta t} + \frac{(\zeta g_{2i+1}^n + u_{i+1/2}g_{1i+1}^n) + ((\zeta g_{2i}^n + u_{i+1/2}g_{1i}^n)}{2\Delta x}$$
$$- \frac{(\zeta g_{2i}^n + u_{i-1/2}g_{1i}^n)) - (\zeta g_{2i}^n + u_{i-1/2}g_{1i-1}^n)}{2\Delta x} - (\zeta + ||u||_\infty)\frac{g_{1i+1}^n - 2g_{1i}^n + g_{1i-1}^n}{2\Delta x} = 0.$$

Remark: In order to enforce the realisability conditions (2.13) for the numerical solutions one needs $g_{0i}^{n+1} \geq 0$ and $|g_{1i}^{n+1}| \leq g_{0i}^{n+1}$ for all i. These properties are directly shown by computing $g_{0i}^{n+1} + g_{1i}^{n+1}$ and $g_{0i}^{n+1} - g_{1i}^{n+1}$. One can show the scheme (4.9) preserves the realisability requirement of the numerical solution under the CFL condition (4.6).

Step 2: the second intermediate step we consider writes

$$(4.10) \qquad \begin{cases} \partial_t g_0 - \partial_\zeta(\dfrac{du}{dt}g_1 + \zeta\partial_x u g_2) = 0, \\[2mm] \partial_t g_1 - \partial_\zeta(g_2\dfrac{du}{dt} + \zeta g_3\partial_x u) = 0. \end{cases}$$

Following the same procedure than for the first intermediate state, the following underlying kinetic model is proposed

$$\partial_t F(\zeta) - \partial_\zeta((\frac{du}{dt}\mu + \zeta\partial_x u\mu^2)F(\zeta)) = 0,$$

with the following corresponding scheme

(4.11)
$$\frac{F_j^{n+1} - F_j^n}{\Delta t} + \frac{b_{j+1/2}F_{j+1}^n + (b_{j+1/2} - b_{j-1/2})F_j^n - b_{j-1/2}F_{j-1}^n}{2\Delta\zeta}$$
$$- ||b||_\infty \frac{F_{j+1}^n - 2F_j^n + F_{j-1}^n}{2\Delta\zeta} = 0,$$

with $b = \frac{du}{dt}\mu + \zeta\partial_x u\mu^2$. The CFL condition associated reads

(4.12)
$$\Delta t_2 \leq \frac{\Delta\zeta}{2(||\frac{du}{dt}||_\infty + \zeta||\partial_x u||_\infty)}.$$

The angular integration of (4.11) leads to the following discretisation for the intermediate state (4.10)

$$\frac{g_{0j}^{n+1} - g_{0j}^n}{\Delta t} + \frac{(\frac{du}{dt}g_{1i+1}^n - \zeta_{j+1/2}\partial_x u g_{2j+1}^n) + (\frac{du}{dt}g_{1j}^n - \zeta_{j+1/2}\partial_x u g_{2j}^n)}{2\Delta\zeta}$$
$$- \frac{(\frac{du}{dt}g_{1j}^n - \zeta_{j-1/2}\partial_x u g_{2j}^n)) + (\frac{du}{dt}g_{1j-1}^n - \zeta_{j-1/2}\partial_x u g_{2j-1}^n)}{2\Delta\zeta}$$
$$- (|\frac{du}{dt}| + ||\zeta||_\infty|\partial_x u|)\frac{g_{0j+1}^n - 2g_{0j}^n + g_{0j-1}^n}{2\Delta\zeta} = 0,$$

(4.13)
$$\frac{g_{1j}^{n+1} - g_{1j}^n}{\Delta t} + \frac{(\frac{du}{dt}g_{2j+1}^n - \zeta_{j+1/2}\partial_x u g_{3j+1}^n) + (\frac{du}{dt}g_{2j}^n - \zeta_{j+1/2}\partial_x u g_{3j}^n)}{2\Delta\zeta}$$
$$- \frac{(\frac{du}{dt}g_{2j}^n - \zeta_{j-1/2}\partial_x u g_{3j}^n) - (\frac{du}{dt}g_{2j-1}^n - \zeta_{j-1/2}\partial_x u g_{3j-1}^n)}{2\Delta\zeta}$$
$$- (|\frac{du}{dt}| + ||\zeta||_\infty|\partial_x u|)\frac{g_{1j+1}^n - 2g_{1j}^n + g_{1j-1}^n}{2\Delta\zeta} = 0.$$

Remark: The scheme (4.13) preserves the realisability domain under the CFL condition (4.12).

Step 3: the third state we consider is the following

$$\begin{cases} \partial_t g_0 = 0, \\ \partial_t g_1 + \frac{g_0 - g_2}{\zeta}\frac{du}{dt} = 0. \end{cases}$$

We choose the following classical scheme for this first model

$$\begin{cases} g_{0ij}^{n+1} = g_{0ij}^n, \\ g_{1ij}^{n+1} = g_{1ij}^n - \Delta t\frac{g_{0ij} - g_{2ij}}{\zeta_j}(\frac{du}{dt})_i. \end{cases}$$

Remark: This scheme preserves the realisability conditions under CFL conditions

$$\Delta t_3 \leq \frac{\zeta}{|\frac{du}{dt}|} \left| \frac{1 + \alpha}{1 - \chi(\alpha)} \right|,$$

where α is defined by (2.11).

Proof. This result is directly obtained by computing $g_{0i}^{n+1} \pm g_{1i}^{n+1}$. $\square$

Remark: The term $\left| \frac{1 + \alpha}{1 - \chi(\alpha)} \right|$ does not tend to zero as α tends to -1. Indeed, using the definition of χ given in (2.11), one can show that $\left| \frac{1 + \alpha}{1 - \chi(\alpha)} \right|$ tends to $1/2$ as α tends to -1.

Step 4: the fourth intermediate step we consider writes

$$\begin{cases} \partial_t g_0 = 0, \\ \partial_t g_1 + \partial_x u(g_1 - g_3) = 0. \end{cases}$$

Following the third step we propose

$$\begin{cases} g_{0i}^{n+1} = g_{0i}^n, \\ g_{1i}^{n+1} = g_{1i}^n + \Delta t(\partial_x u)_i(g_{1i} - g_{3i}). \end{cases}$$

Remark: This scheme preserves the realisability conditions under CFL conditions

$$\Delta t_4 \leq \frac{1}{|\partial_x u|} \left| \frac{1 + \alpha}{\alpha - \chi_2(\alpha)\mathrm{sgn}(\alpha)} \right|.$$

Using the definition of χ_2, we remark that $\left| \frac{1 + \alpha}{\alpha - \chi_2(\alpha)\mathrm{sgn}(\alpha)} \right|$ tends to $1/2$ as α tends to -1.

In order to derive a admissible numerical scheme for the complete model (4.1), we propose to consider the following time semi-discretisation

(4.14) $$U^{n+1} = U^n + \Delta t \sum_{k=1}^N F_k(U^n),$$

where

$$U^{n+1} = \begin{pmatrix} g_0^{n+1} \\ g_1^{n+1} \end{pmatrix}.$$

F_k represents the discretisation proposed for the kth intermediate step and N is the number of intermediate step considered. Equation (4.14) rewrites under the form of a convex combination

(4.15) $$U^{n+1} = \sum_{k=1}^N \frac{1}{N} [U^n + (N\Delta t)F_k(U^n)].$$

Setting $\tilde{\Delta} t = N\Delta t$, one shows that if each intermediate step

$$\tilde{U}^{n+1} = U^n + \tilde{\Delta} t F_k(U^n),$$

preserves the realisability conditions of the numerical solution under CFL condition

$$\tilde{\Delta} t \leq C_k.$$

Therefore the general scheme (4.14) preserves the realisability conditions of the numerical solution under the following CFL condition

$$\Delta t \leq \min_k (\frac{C_k}{N}).$$

The following result is then obtained

THEOREM 4.1. *The general scheme (4.14) preserves the realisability conditions under the following CFL condition*

(4.16) $$\Delta t \leq \frac{1}{4} \min(\Delta t_1, \Delta t_2, \Delta t_3, \Delta t_4).$$

Proof. Each step preserves the realisability conditions under CFL condition. Therefore, by convexity of the admissible set, considering the convex combination (4.15) and using the condition (4.1), we directly obtain that the general scheme (4.14) preserves the realisability conditions under the CFL condition (4.16). □

A splitting technique is used for the collisional terms. More precisely, we start solving the advection terms using the previous schemes, then the following system is considered to compute the contribution of the collisional terms

(4.17)
$$\begin{cases} \partial_t g_0 = \dfrac{1}{\tau}(M_{g_0} - g_0), \\ \partial_t g_1 = -\dfrac{1}{\tau}g_1. \end{cases}$$

An implicit discretisation is considered and the scheme writes

(4.18)
$$\begin{cases} g_0^{n+1} = \dfrac{1}{1 + \dfrac{\Delta t}{\tau}}(\dfrac{\Delta t}{\tau}M_{g_0}^{n+1} + g_0^n), \\ g_1^{n+1} = \dfrac{1}{1 + \dfrac{\Delta t}{\tau}}g_1^n. \end{cases}$$

Therefore, the density n and the temperature T at time t^{n+1} are now required to compute $M_{g_0}^{n+1}$. We recall here the definitions of the density and temperature in terms of g_0

$$n = \int_0^{+\infty} g_0 d\zeta, \qquad T = \frac{1}{3nR}\int_0^{+\infty} g_0 \zeta^2 d\zeta.$$

These quantities are obtained by observing that the quantities $\int_0^{+\infty} g_0 d\zeta$ and $\int_0^{+\infty} g_0 \zeta^2 d\zeta$ are conserved by system (4.17). Indeed, by using the mass and energy conservation properties of the BGK collisional operators, the system (4.17) leads to

$$\partial_t \Big(\int_0^{+\infty} g_0 d\zeta \Big) = 0, \qquad \partial_t \Big(\int_0^{+\infty} g_0 \zeta^2 d\zeta \Big) = 0.$$

Therefore, since we have started to solve the advection terms, the density n and temperature T are already known at time t^{n+1}. They are used to compute $M_{g_0}^{n+1}$ in (4.18). We mention that the same procedure can be used when working with the original kinetic equation.

Different discretisations have been considered in order to compute the velocity u and its space and time derivatives. On the test cases considered, the different choices give very similar results which do not seem sensitive to these choices of discretisation. We mention here that $\frac{du}{dt}$ and $\frac{\partial u}{\partial x}$ are first required to compute the CFL condition to obtain Δt. To achieve such an issue we start combining equation (2.7) and the mass conservation equation (3.20) to obtain

$$\frac{du}{dt} = -\frac{1}{n}\partial_x\left(\int_0^{+\infty} g_2\zeta^2 d\zeta\right).$$

Therefore the following discretisation is considered for the term $\frac{du}{dt}$

$$\left(\frac{du}{dt}\right)_i = -\frac{1}{n_i}\sum_{p=1}^{pf}\zeta_p^2\frac{\bar{h}_{i+1/2p}^n - \bar{h}_{i-1/2p}^n}{\Delta x}\Delta\zeta,$$

where the numerical fluxes writes

$$\bar{h}_{i+1/2p}^n = \frac{1}{2}\left[(g_{2i+1p}^n + g_{2ip}^n) - (g_{1i+1p}^n - g_{2ip}^n)\right].$$

A simple centred scheme is used for the space derivative of u

$$\left(\frac{\partial u}{\partial x}\right)_i^n = \frac{u_{i+1}^n - u_{i-1}^n}{2\Delta x}.$$

Once the time step is obtained we compute g_0 and g_1 at time t^{n+1}. Finally the new velocity at time t^{n+1} is obtained by solving the conservations laws (4.19) using a standard HLL scheme. For the numerical test presented in the next section, an usual Van Leer's slope limiter [27] is used.

4.2. Enforcement of the discrete energy conservation and zero mean velocity condition. In this section, the enforcement of the discrete energy conservation and zero mean velocity condition is discussed. In a recent work [37], a numerical scheme has been proposed to enforce the discrete zero mean velocity condition considering a kinetic equation. However, this strategy does not directly apply in the present case since a nonlinear set of equations (4.1) is considered associated to the realisability conditions (2.13). The enforcement of the discrete energy conservation and the zero mean velocity condition while preserving realisability conditions (2.13) of the numerical solution is particularly challenging and beyond the scope of the present study. However, in order to be able to present numerical results, in this section a correction of the numerical solution is proposed.

In order to enforce the correct energy conservation, we start considering the following conservation laws associated to (4.1)

(4.19)
$$\begin{cases} \partial_t\rho + div_x(\rho u) = 0, \\ \partial_t(\rho u) + div_x(\rho u \otimes u + p - s) = 0, \\ \partial_t E + div_x((E + p - s)u + q) = 0, \end{cases}$$

where E is the total energy. The pressure tensor p, the stress tensor s and the heat flux q expressed in terms of the angular moments read

$$p - s = \frac{m}{2} \int_0^{+\infty} g_2 \zeta^2 d\zeta, \qquad q = \frac{m}{2} \int_0^{+\infty} g_1 \zeta^3 d\zeta.$$

At each time time step, the set of conservation laws (4.19) is numerically solved. Then the numerical solution is corrected by using

$$g_{0p} = \alpha \exp(\beta \zeta_p{}^2) \bar{g}_{0p}, \qquad \forall p \in \{1; ...; pf\},$$

where g_0 is the corrected solution and $\bar{g}_0$ the solution which requires a correction computed with the scheme (4.14). The coefficients α and β are numerically computed such that

$$m \sum_{p=1}^{pf} g_{0p} \Delta \zeta = \rho, \qquad \frac{m}{2} \sum_{p=1}^{pf} g_{0p} \zeta_p^2 \Delta \zeta = E - \frac{\rho u^2}{2},$$

where the quantities E, $\frac{\rho u^2}{2}$ and ρ are known at each time step since the set (4.19) has been numerically solved. This procedure enables the enforcement of the correct energy conservation. As it will be shown in the next section this correction is important for the numerical results, in particular in order to numerically capture shock waves.

In order to enforce the zero mean velocity condition (3.19) at the discrete level, one could think in proposing an adapted discretisation for the source terms which appears in the second equation of (4.1). However, this procedure leads to an unsuitable CFL condition when considering the realisability requirements (2.13) for the numerical solution. Therefore the following correction is proposed based on the resolution of the convex optimisation problem

$$\min_{g_1 \in \mathbb{R}^{pf}} \frac{1}{2} \|g_1 - \bar{g}_1\|_{L^2}^2 = 0,$$

under equality constraint

$$\sum_{p=1}^{pf} g_{1p} \zeta_p \Delta \zeta = 0,$$

where g_1 is the corrected solution and $\bar{g}_1$ the solution before correction given by the scheme (4.14). One observes that this procedure does not enforce the realisable conditions of the numerical solutions. In such unfortunate case, g_1 is simply projected on the realisable set. We also mention that a similar L_2 projection method was proposed in [15], in the context of conservation properties for Boltzmann solvers.

5. Numerical results. In this section, several test cases are presented. Depending on the regime considered, the numerical results obtained with the scheme introduced in the previous part for the angular M_1 moments model in a moving frame, denoted M_1 mobile, are compared either with an exact solution or with a kinetic reference solution. The results are given with and without the correction procedure. In the following, the kinetic solution has been obtained considering a standard

kinetic 1D3V BGK model using an usual Lax-Friedrichs scheme with the second order
Van Leers slope limiter [27]. The results obtained with this scheme are denoted BGK
1D3V. In addition, the results obtained considering a second order HLL scheme for
the Euler equations using the second order Van Leers slope limiter are also given.
These results obtained using this scheme are denoted Euler.

Test 1: Temperature gradient test case in different collisional regimes.

The first test case we study consists in considering a strong temperature gradient
at initial time and studying the temporal evolution of density, velocity and temper-
ature. The initial distribution function is supposed to be a Maxwellian distribution
function defined by

$$f_{ini}(x, v) = \frac{n_{ini}(x)}{(2\pi T_{ini}(x))^{3/2}} \exp\left(-\frac{(v - u_{ini}(x))^2}{2T_{ini}(x)}\right),$$

with

$$n_{ini}(x) = 1, \quad u_{ini}(x) = 0, \quad T_{ini}(x) = 2 - \arctan(x).$$

The space range chosen is $[-40, 40]$, and the velocity range $[-15, 15]^3$. For the present
test case, 400 cells in space and 200^3 cells in velocity have been considered for the
1D3V BGK kinetic approach. Also, 400 cells in space and 200 cells in velocity mod-
ulus have been considered for the M_1 mobile scheme. Finally, 400 cells in space have
been considered for the Euler description.
Neumann boundary conditions are considered, the values in the boundary ghost cells
set to the values in the corresponding real boundary cells.

1.a Fluid regime.
The first regime we consider is the fluid regime. The collisional parameter τ is set equal
to zero. In Figure 5.1, the density, velocity and temperature profiles are displayed
at time $t = 10$ for the kinetic BGK 1D3V scheme in continuous blue, the M_1 mobile
scheme in dashed green, the M_1 mobile scheme with correction in dashed blue and for
the Euler scheme in dashed-point pink. It is observed that all the schemes converge
towards the same solution. This behaviour is expected since working in fluid regime
the distribution remains a Maxwellian distribution function and the three descriptions
give the same solution.

1.b Rarefied regime.
The second regime we consider is a rarefied regime where the collisional parameter τ is
set equal to 1. In Figure 5.2, the density, velocity, temperature and heat flux profiles
are displayed at time $t = 10$ for the kinetic BGK 1D3V scheme in continuous blue, the
M_1 mobile scheme in dashed green, the M_1 mobile scheme with correction in dashed
blue and for the Euler scheme in dashed-point pink. The Euler scheme gives the same
results than in the previous case 1a. This is expected since the description is not
able to distinguish the different regimes. In this case the heat flux is equal to zero.
One observes that M_1 mobile scheme gives close results to the ones obtained with
the kinetic BGK 1D3V scheme. When looking at the heat flux profiles, one observes
that the general trends are qualitatively similar with some notable differences in the
amplitude reached. Since the heat flux is a high order velocity moment, the differences
between the models are particularly visible. The M_1 model is accurate in collisional
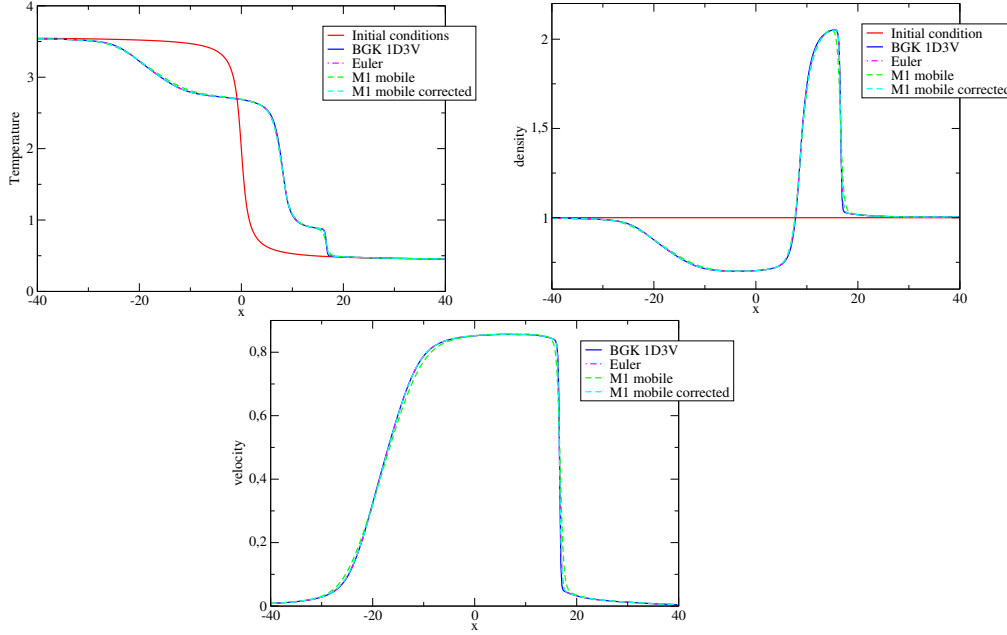
Fig. 5.1: Test 1a - Solution profiles obtained for the temperature gradient test case with $\tau = 0$ at time $t = 10$.

regimes, however as pointed out in [23], it can be inaccurate in collisionless regimes. The differences observed here, are due to the inaccuracy to the M_1 model in rarefied regime.

1.c Non-homogeneous collisional parameter.
When considering realistic physical applications, the collisional parameter varies according to the gas conditions. Therefore, in the third case we consider that the collisional parameter τ is variable in space and is defined by

$$\tau(x) = \frac{1}{2}(\arctan(1 + 0.1x) + \arctan(1 - 0.1x)).$$

In Figure 5.3, the density, velocity, temperature and heat flux profiles are displayed at time $t = 10$ for the kinetic BGK 1D3V scheme in continuous blue, the M_1 mobile scheme in dashed green and for the Euler scheme in dashed-point pink. It is observed that the profiles obtained using the M_1 mobile scheme and the BGK 1D3V scheme are very close. One also observes that even the heat flux profiles are very similar. These results show the interest in using an angular moment model.

Test 2: Sod tube test case in fluid regime

The second test case we study is the Sod tube test case in fluid regime. The initial distribution function is supposed to be a Maxwellian distribution function defined by

$$f_{ini}(x, v) = \frac{n_{ini}(x)}{(2\pi T_{ini}(x))^{3/2}} \exp\left(-\frac{(v - u_{ini}(x))^2}{2T_{ini}(x)}\right),$$
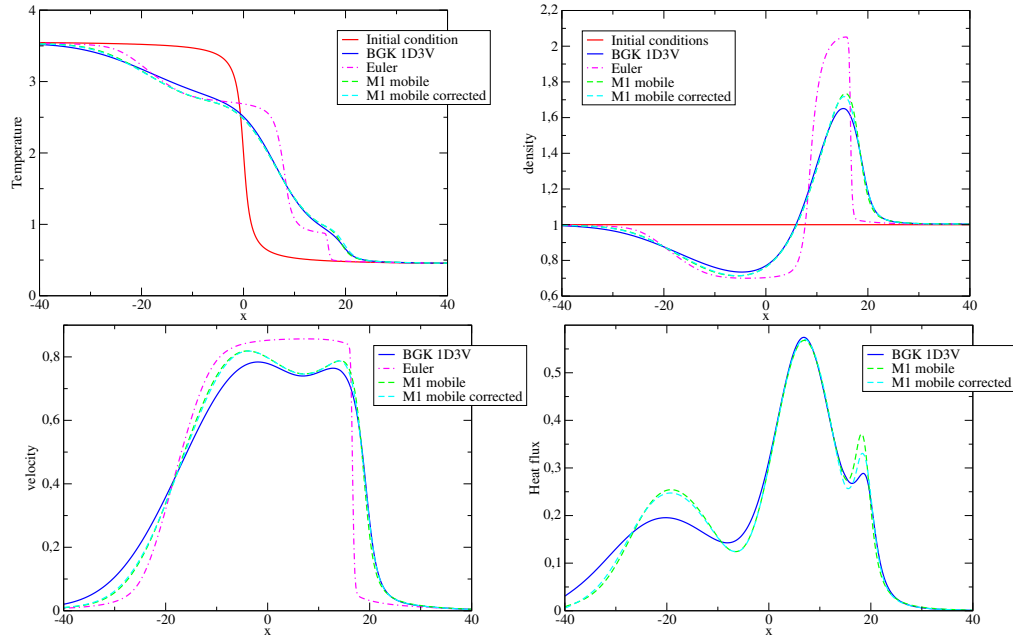
Fig. 5.2: Test 1b - Solution profiles obtained for the temperature gradient test case with $\tau = 1$ at time $t = 10$.
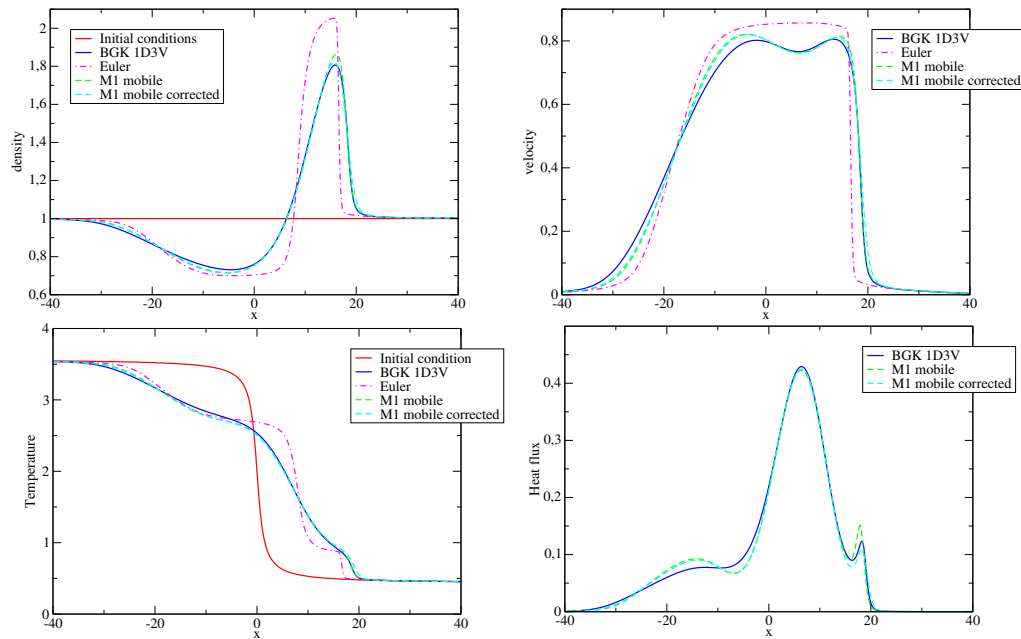
Fig. 5.3: Test 1c - Solution profiles obtained for the temperature gradient test case with variable collisional parameter at time $t = 10$.
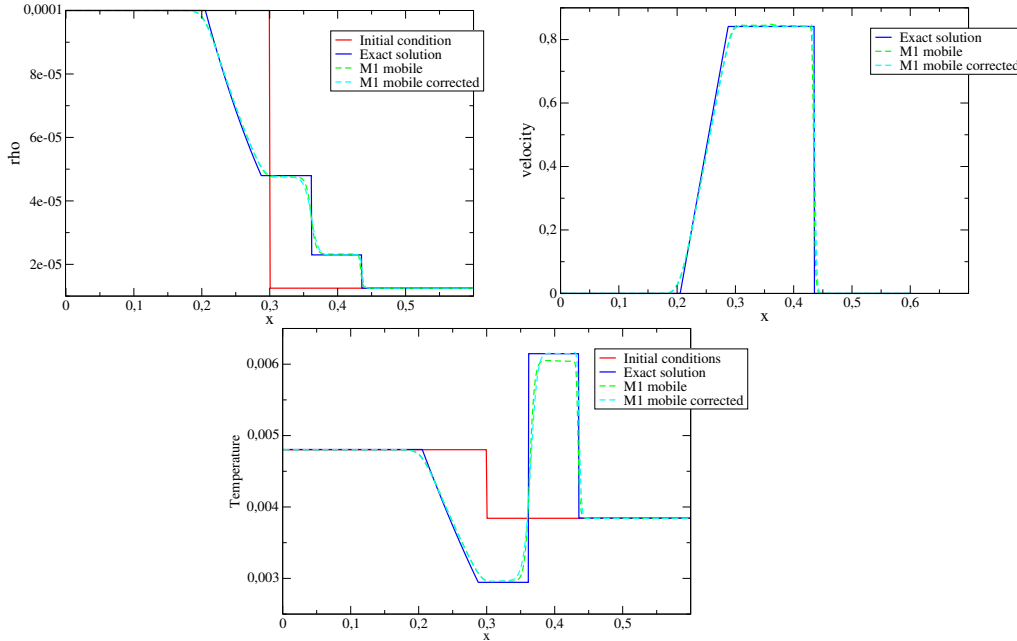
Fig. 5.4: Test 2 - Sod tube test case with $\tau = 0$ at time $t = 7.34 \cdot 10^{-2}$.

with

$$
(n_{ini}(x),\ u_{ini}(x),\ T_{ini}(x)) = \begin{cases} (1.00 \cdot 10^{-4},\ \ 0,\ \ 4.80 \cdot 10^{-3}) & \text{if } x < 0, \\ (1.25 \cdot 10^{-5},\ \ 0,\ \ 3.84 \cdot 10^{-3}) & \text{if } x > 0. \end{cases}
$$

The space range chosen is $[0, 0.6]$, and the velocity range $[-20, 20]^3$. For the present test case, 200 cells in space and 200^3 cells in velocity have been considered for the 1D3V BGK kinetic approach. Also, 200 cells in space and 200 cells in velocity modulus have been considered for the M_1 mobile scheme. Finally, 200 cells in space have been considered for the Euler description. Neumann boundary conditions are considered, the values in the boundary ghost cells are set to the values in the corresponding real boundary cells. For this test case, we consider the fluid regime therefore the collisional parameter τ is set equal to 0. For this test case an exact solution is known, a rarefaction wave, a contact discontinuity and a shock wave appear. In Figure 5.4, the mass density, velocity and temperature solution profiles are displayed at time $t = 7.34 \cdot 10^{-2}$. It is observed that the rarefaction wave (left side) is correctly captured by the M_1 mobile scheme (solution displayed in dashed green). However, one remarks that the shock amplitude is not correctly captured. It has been observed that this incorrect behaviour is due to the wrong discrete energy conservation. Indeed, by using the correction procedure introduced in the previous part the results in dashed blue are obtained, in this case the correct amplitude is recovered. We notice, the importance of the correct discrete energy conservation for capturing shock waves. This point is highlighted in the next test case.

Test 3: Double shock wave test case

The third test case we study is the double shock wave test case in fluid regime. The initial distribution function is supposed to be a Maxwellian distribution function defined by

$$f_{ini}(x,v) = \frac{n_{ini}(x)}{(2\pi T_{ini}(x))^{3/2}} \exp\left(-\frac{(v - u_{ini}(x))^2}{2T_{ini}(x)}\right),$$

with

$$(\rho(x),\ u(x),\ T(x)) = \begin{cases} (1,\ \ 2, 0.4) & \text{if } x < 0, \\ (1, -2, 0.4) & \text{if } x > 0. \end{cases}$$

The space range chosen is $[0,1]$, and the velocity range $[-15,15]^3$. For the present test case, 200 cells in space and 200^3 cells in velocity have been considered for the 1D3V BGK kinetic approach. Also, 200 cells in space and 200 cells in velocity modulus have been considered for the M_1 mobile scheme. Finally, 200 cells in space have been considered for the Euler description. Neumann boundary conditions are considered, the values in the boundary ghost cells are set to the values in the corresponding real boundary cells. For this test case, we consider the fluid regime therefore the collisional parameter τ is set equal to 0. For this test case an exact solution is known, two shock waves are created. In Figure 5.5, the mass density, velocity and temperature solution profiles are displayed at time $t = 0.15$. Similarly as remarked in the previous test case, it is observed that the M_1 scheme does not capture the correct amplitude profile nor the correct shock positions (results in dashed green). The results displayed in dashed blue are obtained using the corrected scheme. It is observed that the correction enables to correctly captures the shock profiles. This example confirms the importance of the discrete energy conservation.

Test 4: Case of large velocity differences

In this test case an initial profile with large velocity differences in the domain is considered. This configuration is problematic for the usual BGK model since a very large and refined velocity grid is required to correctly describe the distribution functions in all the domain [6]. The initial distribution function writes

$$f_{ini}(x,v) = \frac{n_{ini}(x)}{(2\pi T_{ini}(x))^{3/2}} \exp\left(-\frac{(v - u_{ini}(x))^2}{2T_{ini}(x)}\right),$$

with

$$u_{ini}(x) = 20 - 12\arctan(x/4), \qquad (\rho_{ini}(x),\ T_{ini}(x)) = (1, 0.4).$$

The initial velocity profile is displayed in Figure 5.6. The space range chosen is $[-50, 50]$ and one notices the large velocity differences in the domain. For the present test case, 4000 cells in space and $500 \times 10 \times 10$ cells in velocity have been considered for the 1D3V BGK kinetic approach for the velocity range $[-10, 60] \times [0, 5] \times [0, 5]$. The number of points required is particularly expensive and makes the BGK approach particularly unsuitable for this case. Also, 4000 cells in space and only 100 cells for the grid $[0, 5]$ in velocity modulus have been considered for the M_1 mobile scheme. The large difference of number of points required for the M_1 mobile model and for
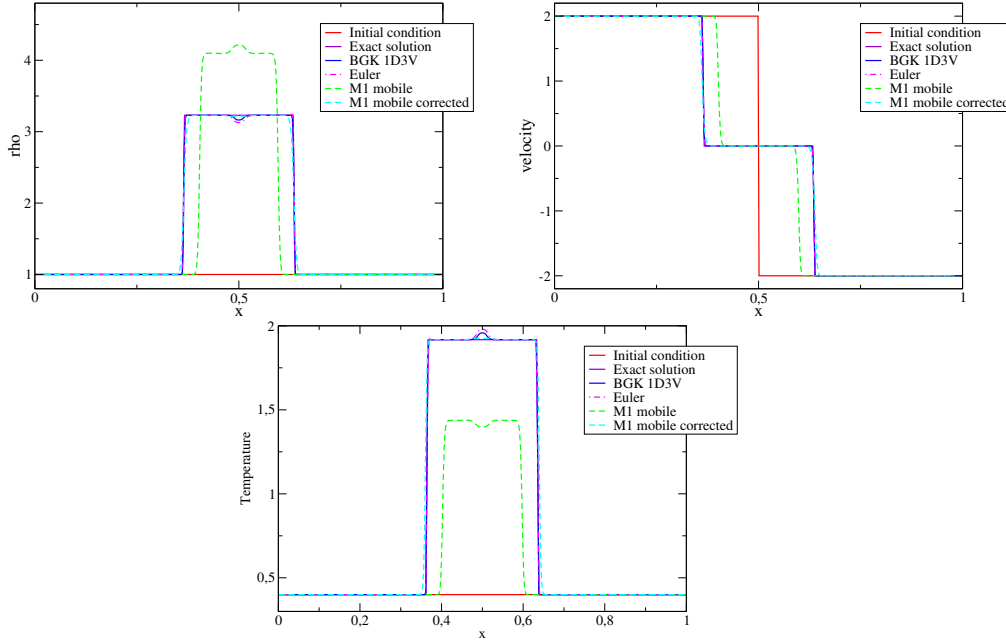
Fig. 5.5: Test 3 - Double shock wave test case with $\tau = 0$ at time $t = 0.15$.
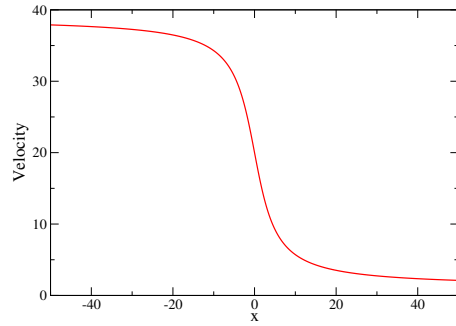

Fig. 5.6: Test 4 - Initial velocity profile.

the BGK model highlights the interest of the approach proposed here. Finally, 4000 cells in space have been considered for the Euler description. Neumann boundary conditions are considered. For this test case, we consider the fluid regime therefore the collisional parameter τ is set equal to 0.

In Figure 5.7, the density, velocity and temperature solution profiles are displayed at time $t = 0.1$ for the kinetic BGK 1D3V scheme in continuous blue, the M_1 mobile scheme in dashed green and for the Euler scheme in dashed-point pink. It is observed that the three profiles obtained are very close. More precisely, when looking at the temperature profile the results obtained with the M_1 mobile are almost identical with the ones obtained with the Euler model. The BGK model remains very close of the two others models despite the huge computational cost involved for this simulation.
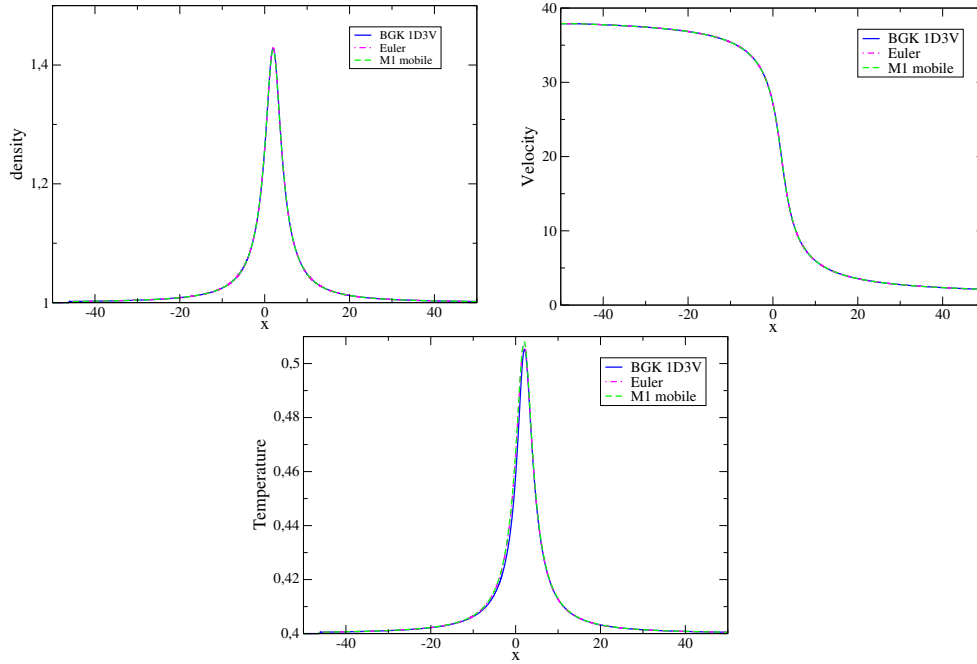
Fig. 5.7: Test 4 - Large velocities test case with $\tau = 0$ at time $t = 0.1$.

In this configuration, these results demonstrate the interest in using the M_1 mobile model, compared to usual kinetic approaches, since accurate results are obtained at much lower numerical costs.

6. Conclusion. In this work, the M_1 angular moments model in the particles mean velocity frame has been derived. Several fundamental properties of the model have been presented. In particular, the importance of working in the mean velocity frame has been highlighted. Indeed, this choice of framework is relevant when considering the Galilean invariance property of angular moments models. The derivation of the associated conservation laws has been detailed in addition to the zero mean velocity condition. A numerical scheme preserving the realisable sets has been proposed and validated with numerical test cases in different collisional regimes. Also, the importance of the correct discrete energy conservation has been emphasised.

As a short term perspective, one needs to derive a numerical scheme enforcing the discrete energy conservation and the zero mean velocity condition. Such an issue is challenging since it should be done preserving the realisable property of the numerical solution. As long term perspective, it would be interesting to study the motion of charged particles. One could consider the electron particle transport working in the ion mean velocity framework. This choice would enable a great simplification of the electron-ion collisional operator and an important step toward the multispecies particle transport for plasma physics applications.

Appendix: derivation of the angular M_1 model in a moving frame (2.5).
In this section, the derivation of the angular M_1 model in a moving frame is detailed. The kinetic equation (2.2) is considered for the angular integration. Introduce a test

function ϕ, we consider the integral

$$\int_c \Big(\partial_t g + div_x((c+u)g) - div_c(\frac{du}{dt}g + \frac{\partial u}{\partial x}cg)\Big)\phi(\zeta)dc = 0.$$

By using the Green formulae and $c = \zeta\Omega$

$$\int_c (\partial_t g + div_x((c+u)g))\phi(\zeta)dc + \int_c (\frac{du}{dt}.g\Omega + \frac{\partial u}{\partial x} : \Omega\otimes\Omega\zeta g)\phi'(\zeta)dc = 0.$$

In spherical coordinates the previous equation leads to

$$\int_\zeta\int_{S^2}(\partial_t g + div_x((c+u)g))\phi(\zeta)\zeta^2 d\Omega d\zeta + \int_\zeta\int_{S^2}(\frac{du}{dt}.g\Omega + \frac{\partial u}{\partial x} : \Omega\otimes\Omega\zeta g)\phi'(\zeta)\zeta^2 d\Omega d\zeta = 0.$$

By using the definitions of the angular moments

$$\int_\zeta (\partial_t g_0 + div_x(\zeta g_1 + u g_0))\phi(\zeta)d\zeta + \int_\zeta (\frac{du}{dt}.g_1 + \frac{\partial u}{\partial x} : \zeta g_2)\phi'(\zeta)d\zeta = 0.$$

Finally by integration by part,

$$\int_\zeta \Big(\partial_t g_0 + div_x(\zeta g_1 + u g_0) - \frac{\partial}{\partial\zeta}\Big[\frac{du}{dt}.g_1 + \frac{\partial u}{\partial x} : \zeta g_2\Big]\Big)\phi(\zeta)d\zeta = 0.$$

This holds true for all test function ϕ then one obtains the first equation of (2.5)

$$\partial_t g_0 + div_x(\zeta g_1 + u g_0) - \frac{\partial}{\partial\zeta}\Big[\frac{du}{dt}.g_1 + \frac{\partial u}{\partial x} : \zeta g_2\Big] = 0.$$

Introduce a test function $\phi\Omega$, we consider the integral

$$\int_c \Big(\partial_t g + div_x((c+u)g) - div_c(\frac{du}{dt}g + \frac{\partial u}{\partial x}cg)\Big)\phi(\zeta)\Omega dc = 0.$$

By using the Green formulae

$$\int_c \Big(\partial_t g + div_x((c+u)g)\Big)\phi(\zeta)\Omega dc + \int_c \frac{\partial\phi(\zeta)\Omega}{\partial c}(\frac{du}{dt}g + \frac{\partial u}{\partial x}cg)dc = 0.$$

Using the fact that

$$\frac{\partial\phi(\zeta)\Omega}{\partial c} = \phi'(\zeta)\Omega\otimes\Omega + \phi(\zeta)\frac{Id - \Omega\otimes\Omega}{\zeta}.$$

Then the second term of the left side of the equation gives

$$\int_c \frac{\partial\phi(\zeta)\Omega}{\partial c}(\frac{du}{dt}g + \frac{\partial u}{\partial x}cg)dc = \int_c \frac{Id - \Omega\otimes\Omega}{\zeta}\frac{du}{dt}g\phi(\zeta)dc + \int_c \frac{Id - \Omega\otimes\Omega}{\zeta}\frac{\partial u}{\partial x}cg\phi(\zeta)dc$$
$$+ \int_c \Omega\otimes\Omega\frac{du}{dt}\phi'(\zeta)g(c)dc + \int_c \Omega\otimes\Omega\frac{\partial u}{\partial x}cg(c)\phi'(\zeta)dc$$

The first term of the right side reads

$$\int_c \frac{Id - \Omega\otimes\Omega}{\zeta}\frac{du}{dt}g\phi(\zeta)dc = \int_\zeta \frac{g_0 Id - g_2}{\zeta}\frac{du}{dt}\phi(\zeta)d\zeta.$$

The second term of the right side writes

$$\int_c \frac{Id - \Omega \otimes \Omega}{\zeta} \frac{\partial u}{\partial x} cg\phi(\zeta)dc = \int_\zeta (\frac{\partial u}{\partial x}g_1 - g_3\frac{\partial u}{\partial x})\phi(\zeta)d\zeta.$$

The third term of the right side leads to

$$\int_c \Omega \otimes \Omega \frac{du}{dt}\phi'(\zeta)g(c)dc = -\int_\zeta \frac{\partial g_2}{\partial \zeta}\frac{du}{dt}\phi(\zeta)d\zeta.$$

The fourth term of the right side gives

$$\int_c \Omega \otimes \Omega \frac{\partial u}{\partial x}cg(c)\phi'(\zeta)dc = -\int_\zeta \frac{\partial \zeta g_3}{\partial \zeta}\frac{\partial u}{\partial x}\phi(\zeta)d\zeta.$$

Finally one obtains the second equation of (2.5)

$$\partial_t g_1 + div_x(\zeta g_2 + u \otimes g_1) - \partial_\zeta\left(g_2\frac{du}{dt} + \zeta g_3\frac{\partial u}{\partial x}\right) + \frac{g_0 Id - g_2}{\zeta}\frac{du}{dt} + \left(\frac{\partial u}{\partial x}g_1 - g_3\frac{\partial u}{\partial x}\right) = 0.$$

REFERENCES

[1] G.W. Alldredge, C.D. Hauck, and A.L. Tits. High-order entropy-based closures for linear transport in slab geometry II: A computational study of the optimization problem. SIAM Journal on Scientific Computing Vol. 34-4 (2012), pp. B361-B391.

[2] S. Benzonie-Gavage and D. Serre. Multi-dimensonal Hyperbolic Partial Differential Equations. Oxford Science Publications.

[3] C. Berthon, C. Buet, J.-F. Coulombel, B. Després, J. Dubois, T. Goudon, J. E. Morel, and R. Turpault. Mathematical models and numerical methods for radiative transfer. Volume 28 of Panoramas et Synthèses (Panoramas and Syntheses(. Société Mathématique de France, Paris, 2009.

[4] C. Berthon, P. Charrier, and B. Dubroca. An HLLC Scheme to Solve The M1 Model of Radiative Transfer in Two Space Dimensions. Journal of Scientific Computing, Vol. 31, No. 3, (2007).

[5] A. Bobylev, J. Carrillo, and I. Gamba. On some properties of kinetic and hydrodynamic equations for inelastic interactions. J. Stat. Phys. 98, 3 (2000), 743773.

[6] S. Brull and L. Mieussens. Local discrete velocity grids for deterministic rarefied flow simulations. J. Comput. Phys., 266(1), 22-46 (2014).

[7] P. Charrier, B. Dubroca, G. Duffa, and R. Turpault. Multigroup model for radiating flows during atmospheric hypersonic re-entry. Proceedings of International Workshop on Radiation of High Temperature Gases in Atmospheric Entry, pp. 103110. Lisbonne, Portugal. (2003).

[8] B. Dubroca, J.-L. Feugeas, and M. Frank. Angular moment model for the Fokker-Planck equation. European Phys. Journal D, 60, 301, (2010).

[9] B. Dubroca and J.L. Feugeas. Entropic moment closure hierarchy for the radiative transfert equation. C. R. Acad. Sci. Paris Ser. I, 329 915, (1999).

[10] B. Dubroca and J.L. Feugeas. Étude théorique et numérique d'une hiéarchie de modèles aux moments pour le transfert radiatif. C. R. Acad. Sci. Paris, t. 329, SCrie I, p. 915-920, (1999).

[11] F. Filbet and T. Rey. A hierarchy of hybrid numerical methods for multi-scale kinetic equation. SIAM J. Sci. Computing, 37 Issue: 3 Pages: A1218-A1247 (2015).

[12] F. Filbet and T. Rey. A Rescaling Velocity Method for Dissipative Kinetic Equations - Applications to Granular Media. J. Comput. Physics, vol 248, pp. 177-199 (2013).

[13] F. Filbet and G. Russo. A Rescaling Velocity Method for Kinetic Equations: the Homogeneous Case. In Proceedings Modelling and Numerics of Kinetic Dissipative Systems (Lipari, 2004), Nova-Science, p. 11.

[14] K.0. Friedrichs and P.D. Lax. Systems of Conservation Equations with a Convex Extension. Proc. Nat. Acad. Sci. USA Vol. 6S, No. 8, pp. 1686-1688, 1971.

[15] I. Gamba and S. Tharkabhushanam. Spectral-Lagrangian methods for collisional models of non-equilibrium statistical states. J. Comput. Physics, vol. 228, Issue 6, 1, pp. 2012-2036 (2009).

[16] M. Gonzalez, E. Audit, and P. Huynh. HERACLES: a three-dimensional radiation hydrodynamics code. AA 464, 429-435 (2007).

[17] T. Goudon and C. Lin. Analysis of the M1 model: well-posedness and diffusion asymptotics. J. Math. Anal. Appl. 402 (2) (2013) 579593.

[18] H. Grad. On the kinetic theory of rarefied gases. Commun. Pure Appl. Math. 2, 331-407 (1949).

[19] E.P. Gross, P.L. Bathnagar, and M. Krook. A Model for Collision Processes in Gases. I. Small Amplitude Processes in Charged and Neutral One-Component Systems. Phys. Rev. 94 (1954), 511.

[20] C.P.T. Groth and J.G. McDonald. Towards physically-realizable and hyperbolic moment closures for kinetic theory. Continuum Mech. Thermodyn. 21, 467-493 (2009).

[21] S. Guisset, S. Brull, B. Dubroca, E. d'Humières, S. Karpov, and I. Potapenko. Asymptotic-preserving scheme for the Fokker-Planck-Landau-Maxwell system in the quasi-neutral regime. Communications in Computational Physics, volume 19, issue 02, pp. 301-328 (2016).

[22] S. Guisset, S. Brull, E. dHumires, B. Dubroca, and V. Tikhonchuk. Classical transport theory for the collisional electronic M1 model. Physica A: Statistical Mechanics and its Applications, Volume 446, Pages 182-194 (2016).

[23] S. Guisset, J.G. Moreau, R. Nuter, S. Brull, E. dHumières, B. Dubroca, and V.T. Tikhonchuk. Limits of the M1 and M2 angular moments models for kinetic plasma physics studies. J. Phys. A: Math. Theor. 48, 335501 (2015).

[24] Philippe Helluy, Michel Massaro, Laurent Navoret, Nhung Pham, and Thomas Strub. Reduced Vlasov-Maxwell modeling. PIERS Proceedings, August 25-28, Guangzhou, 2014, Aug 2014, Gunagzhou, China. pp.2622-2627, 2014.

[25] M. Junk and A. Unterreiter. Maximum entropy moment systems and Galilean invariance. Contin. Mech. Thermodyn. 14 (2002), no. 6, 563576.

[26] L. Landau. On the vibration of the electronic plasma. J. Phys. USSR 10 (1946).

[27] B. Van Leer. Towards the ultimate conservative difference scheme III. Upstream-centered finite-difference schemes for ideal compressible flow. J. Comput. Phys. 23, 3 (Mar. 1977), 263275.

[28] C.D. Levermore. Moment closure hierarchies for kinetic theories. J. Stat. Phys. 83, 1021-1065 (1996).

[29] E.M. Lifchitz and L.P. Petaevski. Kinetic theory. MIR, Moscow (1979).

[30] J. McDonald and M. Torrilhon. An affordable robust moment closures for CFD based on the maximum-entropy hierarchy. J. Comput. Phys. 251, (2013), p. 500-523.

[31] J.G. McDonald and C.P.T. Groth. Towards realizable hyperbolic moment closures for viscous heat-conducting gas flows based on a maximum-entropy distribution. Continuum Mech. Thermodyn. 25, 573-603 (2012).

[32] D. Mihalas and B. W. Mihalas. Foundations of Radiation Hydrodynamics. New York: Oxford University Press, 1984.

[33] G.N. Minerbo. Maximum entropy Eddigton Factors. J. Quant. Spectrosc. Radiat. Transfer, 20, 541, (1978).

[34] S. Mischler and C. Mouhot. Cooling process for inelastic Boltzmann equations for hard spheres, Part II: Self-similar solutions and tail behavior. J. Stat. Phys. 124, 2 (2006), 703746.

[35] I. Muller and T. Ruggeri. Rational Extended Thermodynamics. Springer, New York (1998).

[36] G.C. Pomraning. Maximum entropy Eddington factors and flux limited diffusion theory. J. of Quantitative Spectroscopy and Radiative Transfer, 26 5 385-388 (1981).

[37] T. Rey and C. Tan. An Exact Rescaling Velocity Method for some Kinetic Flocking Models. To appear in SIAM J. Num. Anal.

[38] J.-F. Ripoll. An averaged formulation of the M1 radiation model with presumed probability density function for turbulent flows. J. Quant. Spectrosc. Radiat. Trans. 83 (34), 493517. (2004).

[39] J.-F. Ripoll, B. Dubroca, and E. Audit. A factored operator method for solving coupled radiation-hydrodynamics models. Trans. Theory. Stat. Phys. 31, 531557. (2002).

[40] R. Sanchez and N. J. McCormick. Review of neutron transport approximations. Nucl. Sci. Eng. (United States), 80(4) (1982).

[41] J. Schneider. Entropic approximation in kinetic theory. ESAIM: M2AN, 38 3 (2004) 541-561.

[42] H. Struchtrup. Macroscopic Transport Equations for Rarefied Gas Flows. Springer, Berlin (2005).

[43] M. Torrilhon. Modeling Nonequilibrium Gas Flow Based on Moment Equations. Annual Review Fluid Mech. 48, (2016), p. 429-458.

[44] R. Turpault. A consistent multigroup model for radiative transfer and its underlying mean opacity. J. Quant. Spectrosc. Radiat. Transfer 94, 357371 (2005).

[45] R. Turpault, M. Frank, B. Dubroca, and A. Klar. Multigroup half space moment appproximations to the radiative heat transfer equations. J. Comput. Phys. 198 363 (2004).